



Numerical Study of the Effect of Concentric, Thermally-insulated Insert on Brinkman-Forchheimer Flow and Heat Transfer through a Cylindrical Tube

P.G. Siddheshwar¹, S.B. Ashoka², Om P. Suthar³

¹Department of Mathematics, Bangalore University, Central College Campus, Bangalore-560001, India. E-mail: mathdrpgs@gmail.com

²Department of Computer Science, Government First Grade College, Yedyur, Bangalore – 560 080, India.

³Department of Mathematics, Dr. B.R. Ambedkar National Institute of Technology, Jalandhar, Punjab-144011, India.

*Corresponding author E-mail: ompsuthar@aol.com, dr.ashoksbc@gmail.com, sutharop@nitj.ac.in, ompsuthar@aol.com

Abstract

The system of non-linear algebraic equations arising from the application of the central difference approximation to the fully developed Brinkman-Forchheimer flow equation is solved using the computer assisted continuation method based on the classical, explicit Runge-Kutta method of four slopes. The continuation method is found to be very effective in capturing boundary and inertia effects in the considered flow through porous media. Further, it succeeds in giving the required solution for large values of Forchheimer number when shooting method fails to do so. Heat transport in forced convective flow through the annulus is quantified in terms of the Nusselt number. It is found that the effect of increasing the radius of the inner cylinder is to increase the Nusselt number. The results of fully-developed, non-linear flow and heat transfer through a rectangular channel and a cylindrical porous tube are obtained as limiting cases of the present study.

Keywords: Brinkman, Forchheimer, Annulus, Heat Transfer, Insert, Computer assisted Numerical Method.

1. Introduction

The utility of porous media in practical applications is well known at the present time to merit more than a not-so-detailed exposition (see Nield and Bejan [1], Vafai [2], Rudraiah et al [3]). In the light of the above observation we merely reiterate the advocacy of umpteen number of eminent researchers to have boundary and inertia effects in flow equations of porous media. To cite a few recent works, we draw attention to the work of Skjetne and Auriault [4] that provides new insights on steady, non-linear flow in porous media. Also the work of Calmdı and Mahajan [5] presents the non-linear, non-Darcy equation as an excellent candidate for description of flow in metal foam porous media. Khaled and Vafai [6] draw us from extra-corporeal application situations into corporeal flows. Their [6] work suggests a non-linear flow model for high perfused skeletal tissues. In all these applications, and many more, high flow rate and /or high permeability in porous media warrants the quantification of the departure from Darcy's law in terms of Brinkman friction and super-linear drag, the former arising due to solid boundaries and the latter caused by form drag due to the solid matrix. Restricting our attention to uni-directional flows, we call attention to two extremely important works of Vafai and Kim [7], and Nield et al [8] that deal with forced convection in a channel filled with a porous medium. A steady, uni-directional, non-linear, non-Darcy flow was assumed in these works. The above two works concern exact solutions of the non-linear two-point boundary-value problem arising in the study. The non-linearity in the governing quasi-linear differential equation is a quadratic function of velocity. In literature, the nomenclature attached with this friction is either after the name of Forchheimer [9] or Ergun [10]. We

follow the classic mathematical works and prefer use of the name of Forchheimer to Ergun on reasons of maintaining continuity in nomenclature and not adding to the confusion in literature over different model names. In so far as the Darcy friction and viscous shear is concerned, there is no debate at the present time on having two viscosities in the equation- actual fluid viscosity and effective viscosity (see Lauriat and Prasad [11] and Givler and Altobelli [12]). In the present problem we consider the two non-Darcy effects due to inertia and boundary. Poulikakos and Renken [13] performed a numerical study of boundary and inertia effects on porous medium flow and heat transfer. Parang and Keyhany [14] analysed mixed convection in an annular region considering boundary and inertia effects. Hooman [15, 16] quite recently has published numerical works pertaining to this non-linear flow model in porous media. In the paper we report the solution of the Brinkman-Forchheimer equation for fully developed two-dimensional flow through an annulus using the finite-difference and homotopy continuation methods. Further heat transport in the forced convective flow is also considered.

2. Mathematical Formulation for Flow through a Cylindrical Porous Annulus

The physical system consists of a highly percolative annulus whose cylindrical surface is impermeable to the liquid. It is assumed that the non-Darcy fully developed flow in the medium can be described by the Brinkman-Forchheimer model and so we have

$$\tilde{\mu} \left(\frac{d^2 w}{dr^2} + \frac{1}{r} \frac{dw}{dr} \right) - \frac{\mu}{k} w - \frac{\rho C_F}{\sqrt{k}} w^2 = \frac{dp}{dz}, \quad (1)$$

where $w(r)$ is the axial filter velocity and $p(z)$ is the axial pressure. The other quantities are as explained in the previous section. The boundary conditions for solving Eq. (1) are

$$w = 0 \quad \text{at} \quad r = R_2, R_1. \tag{2}$$

We now non-dimensionalize Eqs.(1)-(2) using the following definition:

$$Z = \frac{z}{R_1}, \quad Y = \frac{r}{R_1}, \quad P = \frac{p}{\mu u_0/R_1}, \quad U = \frac{w}{(-u_0 \frac{dP}{dz})} \tag{3}$$

where u_0 is a characteristic velocity. Substituting Eq. (3) in Eqs (1)-(2), we get

$$\frac{d^2U}{dY^2} + \frac{\delta}{Y} \frac{dU}{dY} - \Lambda Da^2 U - F U^2 = -\Lambda, \tag{4}$$

$$U(Y) = 0 \quad \text{at} \quad Y = \varepsilon, 1, \tag{5}$$

where

$$Da = R_1/\sqrt{K} \text{ (Darcy number),}$$

$$F = C_F \Lambda Re Da \text{ (Forchheimer number),}$$

$$\Lambda = \mu/\tilde{\mu} \text{ (Brinkman number),}$$

$$Re = -\frac{\rho u_0 R_1}{\mu} \frac{dP}{dz} \text{ (Reynolds number) and}$$

$$\varepsilon = R_2/R_1 \text{ (ratio of radii of cylinders).}$$

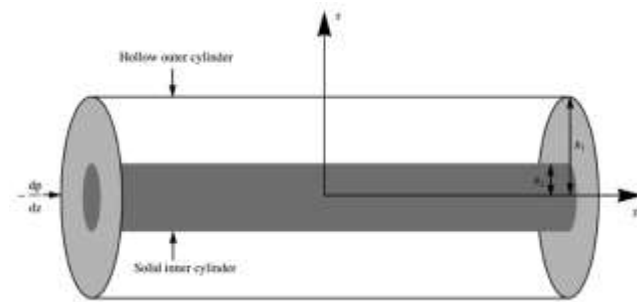


Fig. 1: Schematic of the hollow cylinder with concentric solid cylindrical insert and porous filling.

3. Finite Difference Approximation and Homotopy Continuation Method of Solution

In the method of solution adopted in the paper we need to discretize the interval of interest $[\varepsilon,1]$. We do this by using the discrete points

$$Y_n = \varepsilon + n\Delta Y = \varepsilon + \frac{n(1-\varepsilon)}{N}, \quad n = 0(1)N. \tag{6}$$

In what follows $U(Y_n)$ is denoted by U_n . We first apply the central difference approximation to the first and order second derivatives in equation (5) and this procedure yields:

$$\frac{U_{n+1} - 2U_n + U_{n-1}}{(\Delta Y)^2} + \frac{\delta}{\varepsilon + n\Delta Y} \frac{U_{n+1} - U_{n-1}}{2\Delta Y} - \Lambda Da^2 U_n - F U_n^2 + \Lambda = 0, \quad n = 0(1)N - 1. \tag{7}$$

Rearranging equation (7) we get a system of N non-linear algebraic equations in the form:

$$f_n(U) = F U_n^2 - N^2 \left(1 + \frac{\delta}{2n}\right) U_{n+1} + (2N^2 + A)U_n - N^2 \left(1 - \frac{\delta}{2n}\right) U_{n-1} - \Lambda = 0, \quad n = 0(1)N - 1, \tag{8}$$

with

$$\left. \begin{aligned} U_0 &= 0 && \text{(no - slipcondition),} \\ U_N &= 0 && \text{(no - slipcondition).} \end{aligned} \right\} \tag{9}$$

In equation (8) A is given by

$$A = \Lambda Da^2. \tag{10}$$

Let \underline{U}^* be the unknown solution of the system (9). To obtain this solution we shall later consider a family of problems to be described using a homotopy parameter $p \in [0,1]$. Henceforth, to bring in 'p', we use a suggestive notation $\underline{U}(Y;p)$ in place of $\underline{U}(Y)$ and $f_n(\underline{U};p)$ in place of $f_n(\underline{U})$. With the intention of obtaining $\underline{U}(Y;1) = \underline{U}^*$ from $\underline{U}(Y;0)$, an assumed initial approximation to the system (8), we define the following mapping

$$\underline{G} : [0,1] \times R^N \rightarrow R^N, \tag{11}$$

by

$$\underline{G}(\underline{U};p) = p\underline{F}(\underline{U}) + (1-p)[\underline{F}(\underline{U}) - \underline{F}(\underline{U}(0))] \tag{12}$$

where

$$\underline{G} = [f_0, f_1, \dots, f_{N-1}]^T$$

and

$$\underline{U} = [U_0, U_1, \dots, U_{N-1}]^T.$$

In \underline{U} , the U_n s are actually $U_n(Y;p)$ s, unless otherwise mentioned.

Let us assume $\underline{U}(Y;p)$ is the unique solution of

$$\underline{G}(\underline{U};p) = 0, \tag{13}$$

for each $p \in [0,1]$.

Differentiating equation (13) with respect to p, we get

$$\frac{\partial \underline{G}}{\partial p} + \frac{\partial \underline{G}}{\partial \underline{U}} \frac{\partial \underline{U}}{\partial p} = 0, \tag{14}$$

where

$$\frac{\partial \underline{G}}{\partial \underline{U}}(\underline{U};p) = \begin{bmatrix} \frac{\partial f_0}{\partial U_0} & \frac{\partial f_0}{\partial U_1} & \frac{\partial f_0}{\partial U_{N-1}} \\ \frac{\partial f_1}{\partial U_0} & \frac{\partial f_1}{\partial U_1} & \frac{\partial f_1}{\partial U_{N-1}} \\ \vdots & \vdots & \vdots \\ \frac{\partial f_{N-1}}{\partial U_0} & \frac{\partial f_{N-1}}{\partial U_1} & \frac{\partial f_{N-1}}{\partial U_{N-1}} \end{bmatrix}_{(U_0, U_1, \dots, U_{N-1})}$$

and using equation (12), we have

$$\frac{\partial \underline{G}}{\partial p}(\underline{U};p) = \underline{F}(\underline{U}(Y,0)) = [f_0, f_1, \dots, f_{N-1}]^T_{(U_0[0], U_1[0], \dots, U_{N-1}[0])}.$$

In the above $U_n[0]$ is the assumed initial approximation of system (9). Rearranging equation (14), we get a system of N differential equations:

$$\frac{\partial \underline{U}}{\partial p} = - \left[\frac{\partial \underline{G}}{\partial \underline{U}}(\underline{U};p) \right]^{-1} \frac{\partial \underline{G}}{\partial p}(\underline{U};p). \tag{15}$$

To solve the system (15), subject to condition (9), by the explicit, classical Runge-Kutta method of four slopes we partition the range of p, namely [0,1], into M sub-intervals with the mesh points

$$p_j = j\Delta p = \frac{j}{M}, \quad j = 0(1)M. \tag{16}$$

4. Heat Transport

Local thermal equilibrium and homogeneity are assumed and hence the steady-state thermal energy equation in the absence of heat source terms, axial conduction, and thermal dispersion is:

$$\rho c_p U \frac{\partial T}{\partial z} = \frac{k}{r} \frac{\partial}{\partial r} \left(r \frac{\partial T}{\partial r} \right) \quad (17)$$

It follows from the first law of thermodynamics that

$$\frac{\partial T}{\partial z} = \frac{2q''}{\rho c_p U_m} \quad (18)$$

We now define the mean velocity U and the bulk mean temperature T_m in the following form:

$$U_m = \frac{1}{1-\varepsilon} \int_{\varepsilon}^1 UY dY, \quad T_m = \frac{2}{(1-\varepsilon)U} \int_{\varepsilon}^1 UTY dY.$$

Further, dimensionless variables will now be introduced as (see Hooman [16])

$$\hat{u} = \frac{U}{U_m}, \quad \theta = \frac{T-T_w}{T_m-T_w} \quad (19)$$

The Nusselt number Nu is defined by:

$$Nu = \frac{2q''}{k(T_w-T_m)} \quad (20)$$

As noted by Nield [17], though the local temperature T is a function of both axial and radial coordinates, dimensionless temperature distribution in the fully developed region, θ , is a function of the radial coordinates (Y) only, while the bulk mean temperature is a function of the axial coordinate (z) only. In non-dimensional form eq.17 becomes (when eq.3, eq.19 and eq.20 are used):

$$\frac{d^2\theta}{dY^2} + \frac{1}{Y} \frac{d\theta}{dY} + \hat{u}Nu = 0, \quad (21)$$

where the boundary conditions are as follows

$$\left. \frac{d\theta}{dY} \right|_{Y=\varepsilon} = 0 \quad \text{and} \quad \theta|_{Y=1} = 0. \quad (22)$$

Equation (21) can be solved, using boundary conditions (22), to obtain the following expression for $\theta(Y)$:

$$\theta(Y) = \frac{Nu}{2} \int_Y^1 \frac{1}{Y} (\eta \hat{u} d\eta) dY. \quad (23)$$

Using the compatibility condition,

$$\int_{\varepsilon}^1 Y \hat{u} \theta dY = \frac{1}{2} (1 - \varepsilon) \quad (24)$$

The Nusselt number can be obtained in the form:

$$Nu = \frac{2 \left(\int_{\varepsilon}^1 Y \hat{u} dY \right)^2}{\int_{\varepsilon}^1 Y \hat{u} dY \left[\int_Y^1 \frac{1}{\xi} \left(\int_{\varepsilon}^{\xi} \eta \hat{u}(\eta) d\eta \right) d\xi \right] dY}. \quad (25)$$

The results obtained by solving equations (15), subject to conditions (9), by the Runge-Kutta method are documented in figures 3 - 5. Figure 6 and 7 depict comparison of results of limiting cases of present study. Figures 8-11 show the variation of Nusselt number with different parameters.

5. Results and Discussion

As made known quite explicitly in the introduction it is the intention of the paper to propose a combination of the finite difference and homotopy continuation methods for solving a non-linear, non-Darcy equation with quadratic drag. Heat transport in such a flow is also investigated. Before we embark on a discussion of the solution we note here that the definition of Brinkman and Darcy numbers as used in the paper is inverse of the classical

definitions. We now move on to discuss the results obtained in the paper.

The velocity profiles for different parametric values have been plotted in Figure 2. Figure 2(a) illustrates the fact that the velocity decreases with increase in the value of Darcy number for the annular flow through porous media. The plug velocity is seen in the annulus flow when Da is large. The profile in the case of small Da is parabolic rather than flattened as in plug flow velocity.

Figure 2(b) brings out the effect of the Brinkman number, Λ , on the flow velocity and shows that there is a decrease in velocity with an increase in Λ , as shown by Vafai and Kim [7] and Nield et al. [8]. The boundary effect is captured quite well by the method of solution used in the paper.

In figure 2(c) we clearly see the effect of non-linear form drag on the velocity. The form drag is represented by the Forchheimer number, F . The effect of increasing F is to decrease the velocity, which is similar to the effect of increasing Da . The results of the present paper indicate that the effect of the F on the flow velocity becomes weak for low-percolation media. The excellent results on boundary and inertia effects on flow velocity speak about the utility of the solution procedure in capturing detailed flow features. It is important to mention here that the method succeeds in giving the required solution for large values of F whereas shooting technique, based on Runge-Kutta-Fehlberg45 and modified Newton-Raphson methods, fails in the situation. Figure 3 depicts the effect of ε on the velocity and the expected result of increasing velocity for increasing values of ε can be readily observed.

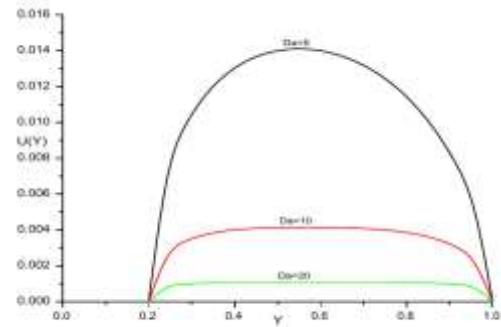
The channel and cylindrical tube results can be obtained from those of the annulus by considering the following BVP:

$$\frac{d^2U}{dY^2} + \frac{\delta}{Y} \frac{dU}{dY} - \Lambda Da^2 U - F U^2 = -\Lambda, \quad (26)$$

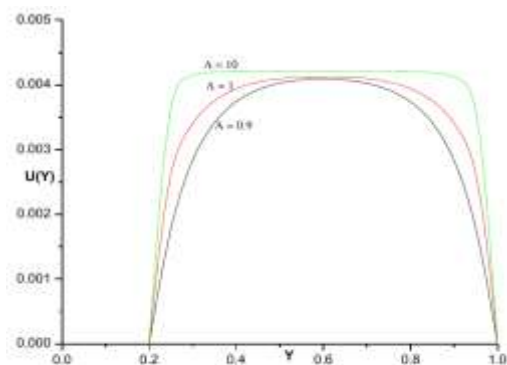
$$U = 0 \quad \text{at} \quad Y = \varepsilon, 1, \quad (27)$$

where

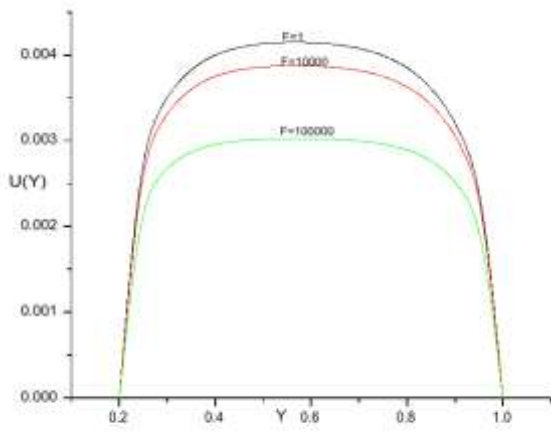
$$(\delta, \varepsilon) = \begin{cases} (0, -1) & \text{for rectangular porous channel,} \\ (1, -1) & \text{for cylindrical porous tube.} \end{cases} \quad (28)$$



(a) $F=2.5, \Lambda=1.2$ with varying Da values.



(b) $F=2.5$ and $Da=10$ with varying Λ values.



(c) $\Lambda = 2.5$ and $Da=10$ with varying F values.

Fig2 (a)-(c): Plots of $U(Y)$ versus Y for the annulus flow ($\epsilon=0.2$)

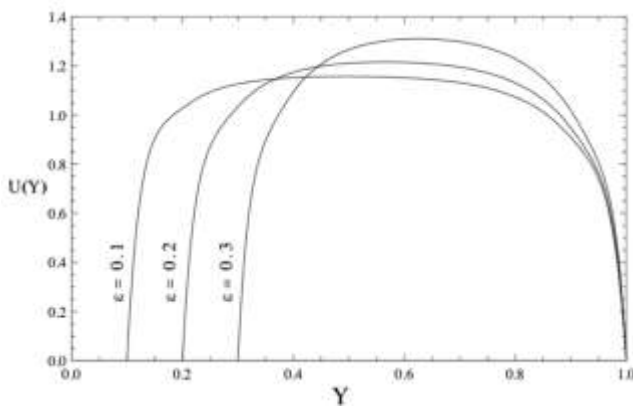


Fig.3: Plot of $U(Y)$ vs. Y for different values of ϵ and for $Da=10$, $F=2.5$ and $\Lambda=1.2$

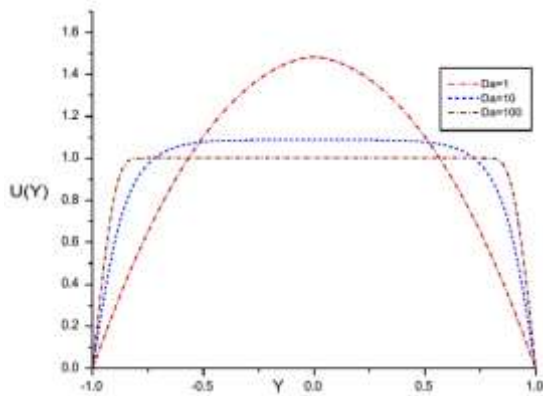


Fig.4: Plot of $U(Y)$ vs. Y for different values of Da and for $F=1$, $\Lambda=1$, $\epsilon=-1$ and $\delta=0$ (rectangular flow of Hooman[15]).

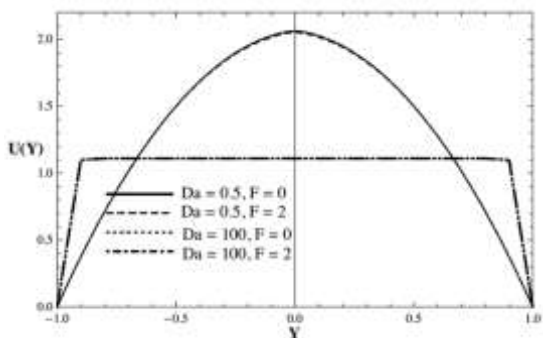


Fig.5: Plot of $U(Y)$ vs. Y for different values of Da and F for $\Lambda=1.2$, $\epsilon=-1$ and $\delta=1$ for cylindrical flow of Hooman and Gurgenci[16].

Figures 4 and 5 show the comparison of the results on velocity with those of Hooman[15] and Hooman and Gurgenci[16] for a rectangular porous channel and cylindrical porous flow. Computations reveal the following general result:

$U_{annulus} < U_{cylinder} \approx U_{rectangular}$ and the same can be seen in each of the figures 2-5. The above result can be attributed to the fact that curvature and concentric cylindrical inserts slow down the fluid in the considered porous medium flow.

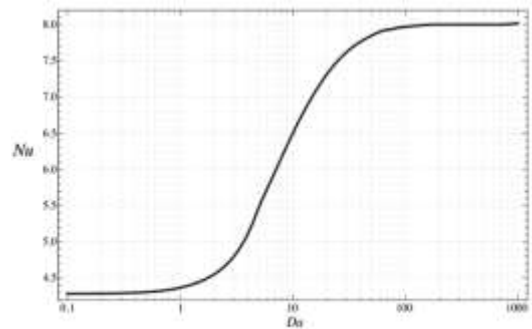
Figure 6(a) depicts the variation of Nusselt number with Da . It can easily be observed that for small values of Da in the range $0.1 \leq Da < 1$, Nusselt number varies insignificantly with Da . A similar observation can be made

on effect of Da in the range $100 \leq Da < \infty$. From the above observations we may thus infer that Nusselt number variation in porous media is significant only in the range $1 \leq Da < 100$. As a consequence we may also conclude that the inclusion of the Forchheimer term is justified in a porous medium whose Da value lies in the range 1 to 100.

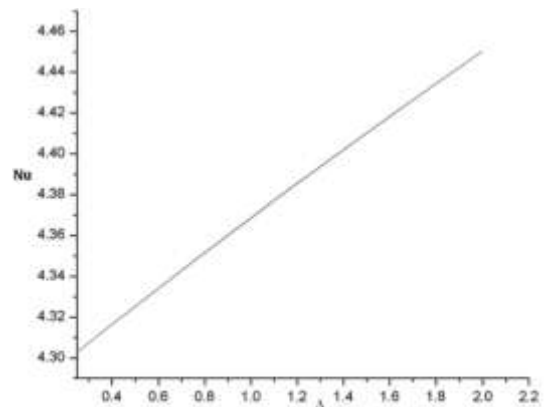
Figure 6(b) illustrates the fact that Nu varies linearly with Λ . This is in keeping with the observation that can be made on the linear variation of $U(Y)$ with Λ . Figure 6(c) reinforces the observation on the Nusselt number variation with Da . Significant changes in Nu with change in F is seen only in the case when $1 \leq F < 1000$. From the Figure we observe that the effect of increasing form drag is to increase the heat transport.

Another important result from the present study is on the variation of Nu with scaled radius of the concentric cylindrical insert (Figure 7). It is apparent that there is less heat transport in a cylinder with no insert in comparison with the corresponding result on Nusselt number when an insert is present. The observation on the plots in the figure 6 are also applicable to cylindrical flows.

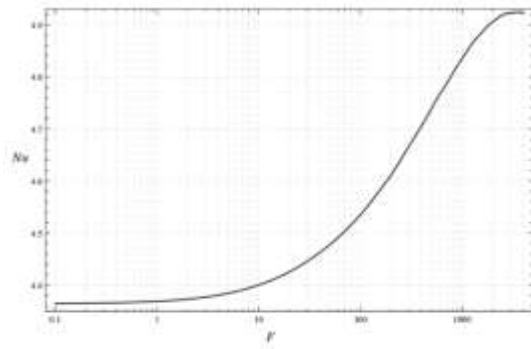
Tables 1 and 2 show close qualitative agreement between the present results on Nusselt number in the limiting cases of Hooman[15], Nield [17] and Gurgenci[16].



(a) Nu vs Da for $\Lambda = 1$ and $F = 1$.



(b) Nu vs Λ for $Da = 1$ and $F = 1$.



(c) Nu vs F for $\Lambda = 1$ and $Da = 1$.
Fig.6 (a)-(c): Plots of Nu for the annulus flow ($\epsilon = 0.2$).

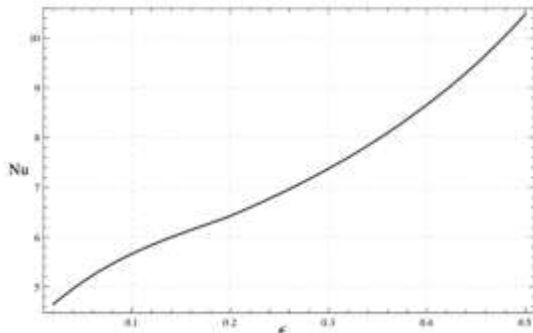


Fig.7: Plot of Nu vs ϵ for fixed values of $Da = 1$, $F = 2$, and $\Lambda = 1$ for a cylindrical annulus ($\delta = 1$).

Table 1: Rectangular Problem-Comparison between present results on Nusselt number with those of Hooman [15] and Nield[17].

Parameters	$\Lambda = 1,$ $F = 0,$ $Da = 0$	$\Lambda = 1,$ $F = 0,$ $Da = 0.5$	$\Lambda = 1,$ $F = 2,$ $Da = 0.5$	$\Lambda = 1,$ $F = 0,$ $Da = 100$
Nu (Present)	4.33108	4.39733	4.33804	5.98708
Hooman & Gurgenci [16]	4.36	—	—	—

Table 2: Cylindrical Problem-Comparison between present results on Nusselt number with those of Hooman and Gurgenci[16].

Parameters	$\Lambda = 1,$ $F = 1$ $Da = 1$	$L = 0.1,$ $F = 1,$ $Da = 1$	$\Lambda = 0.1, F = 1,$ $Da =$ 31.6227766	$\Lambda = 1,$ $F = 1$ $Da = 100$
Nu (Present)	4.146	4.115	5.12886	5.84798
Nield [17]	4.159	4.122	5.129	—
Hooman [15]	4.181	4.131	5.139	5.8935

6. Conclusions

1. The combination of the finite-difference and homotopy continuation methods gives the solution for all permissible values of the parameters of the problem and particularly when the shooting method fails.
2. The presence of thermally-insulated insert is to enhance the velocity and hence the heat transport.
3. There is no need to separately study the forced convection problems of rectangular channel, cylindrical and annulus flows. The results of the first two can be obtained from an annulus flow.

References

[1] Nield, D. A., Bejan, A.: Convection in porous media. Springer Verlag, New York (2013).
 [2] Vafai, K., Hand book of porous media. Taylor and Francis, London (2005).
 [3] Rudraiah, N., Siddheshwar, P. G., Pal, D., Vortmeyer, D.: Non-Darcy effects on transient dispersion in porous media. ASME Proc.,

Nat. Heat Trans. Conf., Houston, Texas, USA (Ed. H. R. Jacobs), HTD – 96 (1) 623 – 629, (1988).
 [4] Skjetne E., Auriault, J. L.: New insights on steady, non-linear flow in porous media. Eur. J. Mech. B/Fluids, 18 131-145, (1999).
 [5] Calmidi, V. V., Mahajan, R. L.: Forced convection in high porosity metal foams. ASME J. Heat Trans., 122 (3), 557-565, (2000).
 [6] Khaled, A. -R. A., Vafai, K.: The role of porous media in modeling flow and heat transfer in biological tissues. Int. J. Heat Mass Trans., 46, 4989-5003, (2003).
 [7] Vafai, K., Kim, S. J.: Forced convection in a channel filled with a porous medium: An exact solution. ASME J. Heat Trans., 111, 1103-1106, (1989).
 [8] Nield, D. A., Junqueira, S.L.M. and Lage, J. L.: Forced convection in a fluid-saturated porous-medium channel with isothermal or isoflux boundaries. J. Fluid Mech 322 201-214, (1996).
 [9] Forchheimer, P. H., Wasserbewegung durch Boden. Ver. Deutsch. Z. Ing 45 1782-1788, (1901).
 [10] Ergun, S.: Flow through packed columns, Chem. Eng. Prog., 48 (2), 89-94, (1952).
 [11] Lauriat, G., Prasad, V.: Natural convection in a vertical porous cavity: A numerical study for Brinkman extended Darcy formulation. J. Heat Trans., 109, 295-330, (1987).
 [12] Givler, R. C., Altobelli, S. A.: A determination of the effective viscosity for the Brinkman – Forchheimer flow model. J. Fluid Mech., 258, 355 -370, (1994).
 [13] Poulikakos, D., Renken, K.: Forced convection in a channel filled with porous medium, including the effect of flow inertia, variable porosity and Brinkman friction. ASME J. Heat Trans. 109, 880-888, (1987).
 [14] Parang, M., Keyhany, M.: Boundary and inertia effect on flow and heat transfer in porous media. Int. J. Heat Mass Trans., 24, 195-203, (1987).
 [15] Hooman, K.: A perturbation solution for forced convection in a porous saturated duct. J. Comput. Appl. Math. 211 (1), 57-66, (2008).
 [16] Hooman, K., Gurgenci, H.: A theoretical analysis of forced convection in a porous saturated circular tube: Brinkman-Forchheimer model. Transport Porous Media, 69 (3), 289-300, (2007).
 [17] Nield, D. A.: A note on a Brinkman-Brinkman forced convection problem. Transport Porous Media, 64, 185-188, 2006.
 [18] Burden, R. L., Faires, J. D.: 7th Edition, Numerical Analysis. Thomson, U. K. (2001).